Geodetic Signature Produced by Different Sources in a Gravitational Layered Earth Model

JOSÉ FERNÁNDEZ[(1)], TING-TO YU[(2)] AND JOHN B. RUNDLE[(3)]

(1) Instituto de Astronomía y Geodesia (CSIC-UCM), Fac. CC. Matemáticas, Ciudad Universitaria, 28040, Madrid, Spain.
(2) Institute of Earth Science, Academia Sinica, P.O. Box 1-55, Nankang, Taipei, Taiwan.
(3) Cooperative Institute for Research in Environmental Sciences, University of Colorado, Boulder, CO 80309, USA.

ABSTRACT. *We describe theoretical and computational methods developed by our group for the calculation of displacement, gravity and potential changes resulting from different sources (representing magma bodies and faults) in elastic-gravitational and viscoelastic-gravitational layered media. The existing codes corresponding to the models are also presented with the information about how they can be obtained for scientific use. The results obtained and work currently in progress are also described in this paper.*

1. DEFORMATION MODEL.

We are mainly interested in computation of gravity and potential changes and displacement on the Earth's surface due to different sources (different kind of magmatic intrusions and faults) in the crust/lithosphere. A model of layered half-space including an ambient gravitational field and representing the Earth for near field problems is considered. This half-space is an elastic medium where a source of perturbation is placed. The equations to be solved that represent the coupled elastic-gravitational problem for a stratified half-space of homogeneous layers are (*Love*, 1911; *Rundle*, 1980)

$$\nabla^2 \boldsymbol{u} + \frac{1}{1-2\sigma}\nabla\nabla\cdot\boldsymbol{u} + \frac{\rho_0 g}{\mu}\nabla(\boldsymbol{u}\cdot\boldsymbol{e}_z) - \frac{\rho_0}{\mu}\nabla\phi - \frac{\rho_0 g}{\mu}\boldsymbol{e}_z\nabla\cdot\boldsymbol{u} = 0$$

$$\nabla^2\phi = -4\pi\rho_0 G_0 \nabla\cdot\boldsymbol{u} \qquad (1)$$

where $\boldsymbol{u}$ is the perturbed displacement vector in the deformed cylindrical coordinate system (r, θ, z), ϕ is the gravitational potential in this coordinate system, $\boldsymbol{e}_r$, $\boldsymbol{e}_\theta$, $\boldsymbol{e}_z$ are the unit vectors, σ is Poisson's ratio, ρ_0 is the density and μ is the rigidity.

Rundle (1980) obtained and solved the equations (1), using the propagator matrix technique (*Thomson*, 1950; *Haskell*, 1953; *Gilbert and Backus*, 1966) to obtain the surface solutions (potential and gravity changes and deformation). *Rundle* (1981a) developed the numerical formulation needed to compute these perturbations for the case of a single layer in welded contact with an infinite half-space. Expressions in the case of two layers may be seen in *Fernández* (1992) and *Fernández and Rundle* (1994a,b), expressions for media composed of three layers have been obtained by *Fernández and Díez* (1995), and more recently, *Fernández et al.* (1997) give the appropriate numerical formulation for a media composed of up to four layers over half-space.

1.1 Solution to the Layered Half Space Problem.

Rundle (1980) used a polar coordinate system (r, θ, z) with the z axis oriented down into the medium at the surface of a layered, elastic-gravitational half space. The elastic module in the *nth* layer are denoted by λ_n and μ_n and the density by ρ_n, see Figure 1.

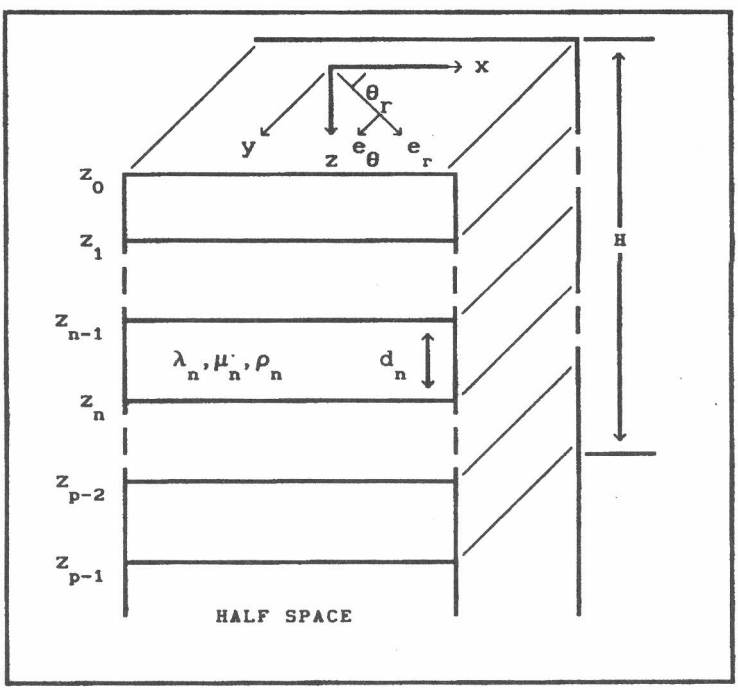

Figure 1. General layered half-space (after Fernández and Rundle, 1994a).

The displacement in the *nth* layer is

$$u^n = \sum_{m=0}^{\infty} \int_0^{\infty} kdku_m^n \,, \tag{2}$$

where u_m^n is given by

$$u_m^n = x_m^n \boldsymbol{P}_m + y_m^n \boldsymbol{B}_m + z_m^n \boldsymbol{C}_m \,. \tag{3}$$

The same formulation is applied to obtain similar expressions for the normal tractions across a plane

$$T^n = \sum_{m=0}^{\infty} \int_0^{\infty} \{ X_m^n \boldsymbol{P}_m + Y_m^n \boldsymbol{B}_m + Z_m^n \boldsymbol{C}_m \} kdk \,, \tag{4}$$

the potential

$$\phi^n = \sum_{m=0}^{\infty} \int_0^{\infty} \omega_m^n J_m(kr) e^{im\theta} kdk \,, \tag{5}$$

and the quantity

$$Q^n = \sum_{m=0}^{\infty} \int_0^{\infty} q_m^n J_m(kr) e^{im\theta} kdk \,. \tag{6}$$

The problem can be divided into two separate parts, the ***R*** problem (that includes the $x^n{}_m$, $y^n{}_m$, $q^n{}_m$, $\omega^n{}_m$ terms), and the ***L*** problem (that includes the $z^n{}_m$ terms). The solutions to these problems are given by *Rundle* (1980) (equations (88)-(96)). We will not examine the ***L*** problem any further because its solution is the same as for the purely elastic case solved by *Singh* (1970) and tabulated by *Rundle* (1980). The integration kernels $x_m{}^1(0)$, $y_m{}^1(0)$, $q_m{}^1(0)$ and $\omega_m{}^1(0)$ are given as a function of the characteristics of the medium's layers, through matrix *[E]* and a vector *[F]* as

$$x_m^1(0) = E_{11} A_{mp} + E_{13} B_{mp} + E_{15} D_{mp} - (F_m)_1, \tag{7}$$

$$y_m^1(0) = E_{21} A_{mp} + E_{23} B_{mp} + E_{25} D_{mp} - (F_m)_2, \tag{8}$$

$$\omega_m^1(0) = E_{51} A_{mp} + E_{53} B_{0p} + E_{55} D_{mp} - (F_m)_5, \tag{9}$$

$$q_m^1(0) = E_{61} A_{mp} + E_{63} B_{mp} + E_{65} D_{mp} - (F_m)_6. \tag{10}$$

The matrix *[E],* a product of propagator matrices (layer matrices), is obtained using the solutions of the infinite space problem (*Rundle*, 1980). Vector $[F_m]$ is a product of layer matrices with the jump discontinuity vector $[D_m]$. Matrix *[E]* is given by

$$[E] = [a^1] \cdot [a^2] \cdots [a^{p-1}] \cdot [Z^p(H)], \tag{11}$$

where $[a^n]$ is the layer matrix (propagator matrix) defined by (*Rundle*, 1980),

$$[a^n] = [Z^n(-d_n)] \cdot [Z^n(0)]^{-1}. \tag{12}$$

The elements of the matrix $[Z^n(z)]$ are functions of k given by *Rundle* (1980, 1982a) and *Fernández* (1992). The vector $[F_m]$ is defined by the product

$$[F_m] = [a^1] \cdot [a^2] \cdots [a^{s1}] \cdot [D_m], \tag{13}$$

where a new layer boundary is introduced at depth c corresponding to the depth of the intrusion $z_{s1} = c$, and s_1 corresponds to the division of the layer where the intrusion is located. $[D_m]$ is the jump discontinuity vector for $z=c$, see *Rundle* (1980) for various examples. The coefficients A_{0p}, B_{0p} and D_{0p} are also given by *Fernández and Rundle* (1994a) in their equations (10)-(15).

1.2 Existence of a top water layer.

The presence of a top water layer in these calculations necessarily modifies the boundary conditions taken into account at the surface (*Rundle*, 1982a). Instead of requiring null elastic traction for $z = 0$ (*Rundle*, 1980) the change of tractions must be considered to be caused by the redistribution of water as a consequence of the deformation. Thus the vertical component of traction in surface z=0, $T_z(0)$, changes and affects the definition of the integration kernels in the equations as is explained by *Rundle* (1982a) and *Fernández et al.* (1997). Examples of sea level changes computations can be found in both of those papers.

1.3 Magmatic Intrusion case.

For a magmatic intrusion, considered as a point mass M placed suddenly at a depth c, the source functions would be those resulting from the interaction between the mass M and the ambient gravity field, equations, and those which reflect the effects caused by the pressurization of the magmatic chamber due to overfilling or temperature changes, and which are given by *Rundle* (1980, 1982a). *Rundle* (1980, 1982a) obtained a unique general solution at z=0 completed by *Fernández et al.* (1997) as

$$\boldsymbol{u} = M \int_0^\infty [\, x_0^1(0)\boldsymbol{P}_0 + y_0^1(0)\boldsymbol{B}_0 \,]kdk\,, \qquad \text{(displacement)} \qquad (14)$$

$$\phi = M \int_0^\infty \omega_0^1(0)\, J_0(kr)kdk, \qquad \text{(potential change)} \qquad (15)$$

$$\delta g = -\frac{d\phi}{dz} = -M \int_0^\infty q_0^1(0) J_0(kr) k dk + \beta_0 u_z, \qquad \text{(gravity change)} \qquad (16)$$

$$t(r) = \frac{\partial u_z}{\partial r} = -M \int_0^\infty x_0^1(0) J_1(kr) k^2 dk \qquad \text{(tilt)} \qquad (17)$$

$$\varepsilon_z = \left(\frac{\partial u_z}{\partial z}\right)(r) = \frac{\lambda_1}{\lambda_1 + 2\mu_1} \int_0^\infty y_0^1(0) J_0(kr) k^2 dk \qquad \text{(and vertical strain)} \qquad (18)$$

where $\boldsymbol{P}_0$ and $\boldsymbol{B}_0$ are vector functions that are given in terms of the Bessel function of the first kind of order zero $J_0(kr)$, and $\beta_0 = 4\pi G\rho_0$, with ρ_0 being the density of the first layer. This solution can be shown to be unique (*Rundle*, 1982).

1.4 Rectangular dipping fault case.

We have also applied this model to compute deformation produced by faulting (see e.g., *Rundle*, 1978, 1980; 1981a, 1981b, 1982b, *Thatcher and Rundle*, 1984; *Yu*, 1995; *Fernández et al.*, 1996a, 1996b; *Yu et al.*, 1996a, 1996b; *Yu and Cheng*, 1997). We present briefly some particularities of the computations on these cases and the equations.

1.4.1 Reduced Problem.

Rundle (1981a) found that for displacements resulting from a dip slip event in a layered elastic-gravitational medium, self-gravitation effects arising from the non-zero value of G_0, the gravitational constant, were generally much smaller

than gravitational effects relating to the surface acceleration, g. As $z \rightarrow \pm\infty$, all perturbed quantities are presumed to tend to zero, so setting $G_0 = 0$ implies ϕ is constant. Making use of this, *Rundle* (1981b) obtain the equations

$$\nabla^2 \boldsymbol{u} + \frac{1}{1-2\sigma}\nabla\nabla\cdot\boldsymbol{u} + \frac{\rho_0 g}{\mu}\nabla(\boldsymbol{u}\cdot\boldsymbol{e}_z) - \frac{\rho_0 g}{\mu}\boldsymbol{e}_z\nabla\cdot\mathrm{u} = 0 \qquad (19)$$

and, using the same techniques outlined in *Rundle* (1980) obtain the corresponding solutions. The advantage of this formulation is the computational pattern that increases the efficiency using a 4x4 matrix problem instead of 6x6 problem. *Rundle* (1981b) found that using the reduced system makes little differences in terms of accuracy computing displacements, and is clearly advantageous.

1.4.2 Thrust fault.

The appropiate source functions (D_m), derived by *Ben Menahem and Singh* (1978) for the six elementary displacement dislocation, are given by *Rundle* (1980). He used the notation of *Singh* (1970) where *(jk)* refers both to the direction of the force system and the normal to the plane across which it is applied. They are given by *Rundle* (1980, 1981a) for a thrust fault dipping of angle ψ. Using this source functions we obtain the expressions for the displacement expressed as

$$\boldsymbol{u} = \frac{H(t)}{4\pi}\int_0^W d\xi \int_{-L}^{L} d\zeta U(\xi,\zeta)\int_0^{\infty}\Big[\Big(x_0^1(0)\boldsymbol{P}_0 + x_2^1(0)\boldsymbol{P}_2 + y_0^1(0)\boldsymbol{B}_0 + y_2^1(0)\boldsymbol{B}_2 + z_2^1(0)\boldsymbol{C}_2\Big)\sin 2\psi$$

$$-\Big(x_1^1(0)\boldsymbol{P}_1 + y_1^1(0)\boldsymbol{B}_1 + z_1^1(0)\boldsymbol{C}_1\Big)\cos 2\psi\Big]kdk \qquad (20)$$

and, finally (***Rundle***, 1981a; *Fernández et al.*, 1996a, 1996b)

$$u_z = \frac{H(t)}{4\pi}\int_0^W d\xi \int_{-L}^{L} d\zeta U(\xi,\zeta)\int_0^\infty \Big[\Big(x_0^1(0)J_0(kr) + x_2^1(0)J_2(kr)\cos 2\theta\Big)\sin 2\psi + x_1^1(0)J_1(kr)\sin\theta\cos 2\psi\Big]kdk,$$

$$u_x = \frac{H(t)}{4\pi}\int_0^W d\xi \int_{-L}^{L} d\zeta U(\xi,\zeta)\int_0^\infty \Big[\big(\varepsilon_1\sin 2\psi + \varepsilon_2\cos 2\psi\big)\cos\theta + \big(\varepsilon_3 \sin 2\psi - \varepsilon_4 \cos 2\psi\big)\sin\theta\Big]kdk, \quad (21)$$

$$u_y = \frac{H(t)}{4\pi}\int_0^W d\xi \int_{-L}^{L} d\zeta U(\xi,\zeta)\int_0^\infty \Big[\big(\varepsilon_1\sin 2\psi + \varepsilon_2\cos 2\psi\big)\sin\theta - \big(\varepsilon_3 \sin 2\psi - \varepsilon_4 \cos 2\psi\big)\cos\theta\Big]kdk,$$

where

$$\varepsilon_1 = -\left[y_0^1(0)J_1(kr) + \left(z_2^1 \frac{J_1(kr)+J_3(kr)}{2} - y_2^1(0)\frac{J_1(kr)-J_3(kr)}{2}\right)\cos 2\theta\right], \quad (22)$$

$$\varepsilon_2 = \left(y_1^1(0)\frac{J_0(kr)-J_2(kr)}{2} + z_1^1(0)\frac{J_0(kr)+J_2(kr)}{2}\right)\sin\theta, \quad (23)$$

$$\varepsilon_3 = \left(y_2^1(0)\frac{J_1(kr)+J_3(kr)}{2} - z_2^1(0)\frac{J_1(kr)-J_3(kr)}{2}\right)\sin 2\theta, \quad (24)$$

$$\varepsilon_4 = \left(y_1^1(0)\frac{J_0(kr)+J_2(kr)}{2} + z_1^1(0)\frac{J_0(kr)-J_2(kr)}{2}\right)\cos\theta. \quad (25)$$

Equations (23)-(25) must replace equations (5)-(7) in *Fernández et al.* (1996a) and equations (21)-(23) in *Fernández et al.* (1996b) which present some minor misprints.

1.4.3 Strike slip fault.

The source functions (D_m) are given by *Rundle* (1980) for a strike slip fault plane inclined at an angle ψ to the horizontal.The displacement at the surface may be written (*Yu* ,1995; *Yu et al.* 1996a,1996b)

$$\boldsymbol{u} = \int_0^\infty kdk \{[x_2^1(0)P_2 + y_2^1(0)B_2 + z_2^1(0)C_2]\cos\psi + [x_1^1(0)P_1 + y_1^1(0)B_1 + z_1^1(0)C_1]\sin\psi\} \tag{26}$$

and, substituting $\boldsymbol{P_m}$, $\boldsymbol{B_m}$ and $\boldsymbol{C_m}$, replacing $e^{im\theta}$ and $ie^{im\theta}$ by $cosm\theta$ and $-sinm\theta$, respectively, to obtain the real part, and splitting the displacement vector into its three components, we obtain

$$u_r = \int_0^\infty kdk \left\{\left[\tfrac{1}{i}y_1^1(0)\left(\tfrac{\partial}{\partial kr}\right)J_1(kr) + z_1^1(0)\left(\tfrac{1}{kr}\right)J_1(kr)\right]\cos\theta\cos\psi - \left[y_2^1(0)\left(\tfrac{\partial}{\partial kr}\right)J_2(kr) + \tfrac{1}{i}z_2^1(0)\left(\tfrac{1}{kr}\right)J_2(kr)\right]\sin 2\theta\sin\psi\right\} \tag{27}$$

$$u_\theta = -\int_0^\infty kdk \left\{\left(\frac{1}{i}y_1^1(0)\left(\tfrac{1}{kr}\right)J_1(kr) + z_1^1(0)\left(\tfrac{\partial}{\partial kr}\right)J_1(kr)\right)\sin\theta\cos\psi + \left(y_2^1(0)\left(\tfrac{2}{kr}\right)J_2(kr) + \tfrac{1}{i}z_2^1(0)\left(\tfrac{\partial}{\partial kr}\right)J_2(kr)\right)\cos 2\theta\sin\psi\right\} \tag{28}$$

$$u_z = -\int_0^\infty kdk \left\{\tfrac{1}{i}x_1^1(0)J_1(kr)\sin\theta\sin\psi - x_2^1(0)J_2(kr)\sin 2\theta\cos\psi\right\} \tag{29}$$

solution to the elastic-gravitational problem of a point nucleus of strike slip in an elastic-gravitational layer over an elastic-gravitational half space. From u_r, u_θ we

can compute u_x, u_y in a easy way. To calculate the displacement due to a finite fault plane we only need to integrate (27)-(29) over the source region, as in (21).

1.4.4 Introduction of viscoelasticity.

We can compute the time dependence displacement following *Rundle* (1982b). After the elastic Green's functions are computed, the correspondence principle of linear viscoelasticity is applied. This requires that the elastic quantities λ and μ in each component of the elastic solution (each here represented by $u(t)$) be replaced by their Laplace transformed quantities $s\overline{\lambda}(s)$ and $s\overline{\mu}(s)$ to obtain $\overline{u}(s)$ where the bar signifies the Laplace transformed quantity and s is the parameter conjugate to time. $\overline{u}(s)$ is then inverted to give $u_v(t)$, the solution to the viscoelastic problem. The technique used to perform the inversion involves the Prony series where the function $u_v(t)$ is approximated by a function $u_v^*(t)$ comprised of a series of decaying exponentials (*Schapery*, 1961; *Cost*, 1964). This approximation method has the advantage of smooth time domain results in the time interval required and involves as few function evaluations as possible. The error obtained using the numerical method is thus minimized. $u_v^*(t)$ can then be integrated over the source region to obtain the required solution.

2. SOME RESULTS.

Our results on computing displacements and gravity changes due to a point magma intrusion in layered elastic-gravitational media show that (*Fernández and Rundle*, 1994a, 1994b) variations in elastic moduli have a much more significant effect than variations in reference density on both the surface displacements and

gravity changes. It can be seen in Figures 2 and 3, obtained using the media described in Table 1. Deviations of the half-space displacements in the layered medium from the homogeneous half-space are clearly due to variations in strain arising from changes in the elastic moduli. However, variations in surface gravity are also influenced far more by changes in moduli than by changes in density, implying that changes in density due to volumetric dilatation are significantly larger than Bouguer effects caused by changing the layer reference densities. Our results clearly indicate that models with uniform density and moduli, or even a single layer over a half-space, may be too simple to adequately model observed gravity and deformation changes in volcanic regions.

The effect of the gravity field has been taken into account, and it has been found that it can be fundamental to adjust and to explain properly gravity changes measured in active zones (*Fernández et al.*, 1997). It is clearly shown in Figure 4. This figure shows vertical and horizontal deformation, tilt and gravity changes due to a center of expansion (ce) and a point mass (mp), both of them located at 6 km depth in the Lanzarote crustal model composed of two layers over the mantle (*Fernández and Rundle*, 1994a). The contribution to the total effect (in the cases of displacement and tilt) of the intrusion mass (mp in Figure 4) is almost null compared to the contribution made by the pressure changes (ce in Figure 4). Suppressing the effect of the gravitational field we get gravity change and deformation values similar to those displayed in Figure 4 for a center of expansion. It is seen that gravitational effects are not significant for displacements and tilt at the surface, in agreement with *Rundle* (1980), but this is not the case for surface gravity change, where the mass of the intrusion is significant and the effect may be very important. Therefore it is seen that gravity field consideration in the model is important for modeling and understanding observed gravity change data. This effect is also important if we consider viscoelastic properties for the medium. *Hofton et al.*

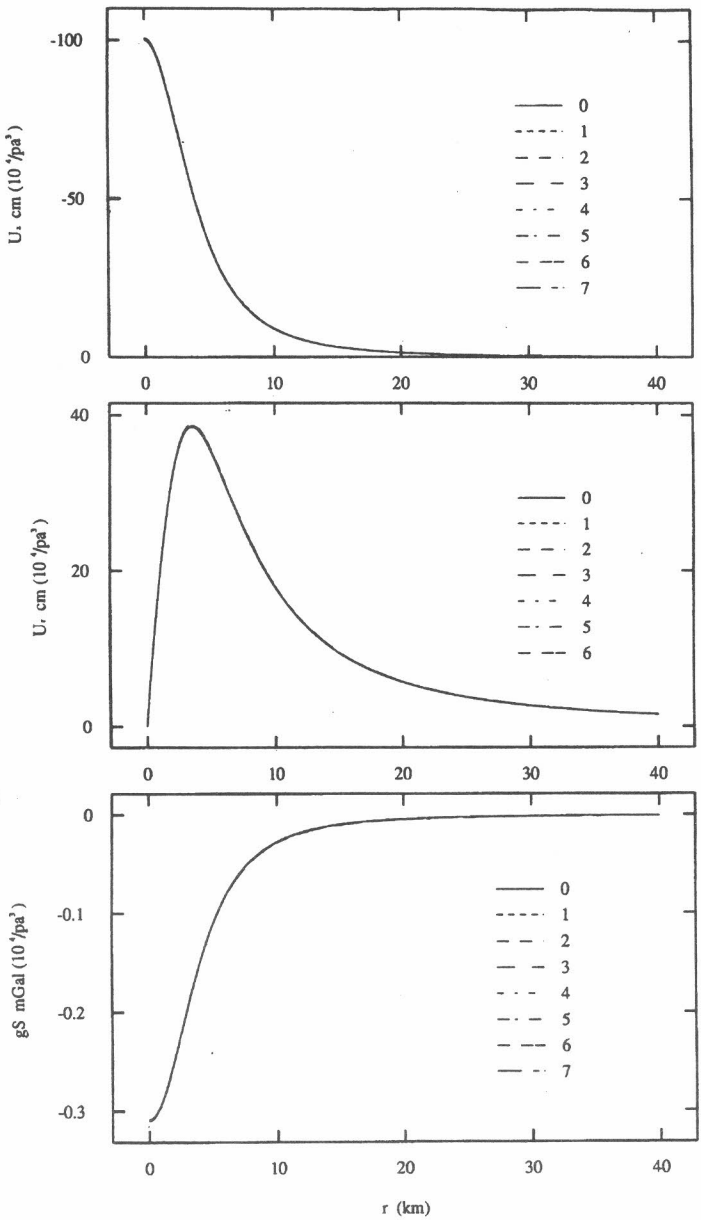

Figure 2. Vertical deformation U_z, radial deformation U_r and surface gravity change gS due to a center of expansion of strength pa^3, where p is the pressure in bars and a the radius in km, located at 5 km depth (layer 1) in media 0 to 7 described in Table 1 (Fernández and Rundle, 1994a).

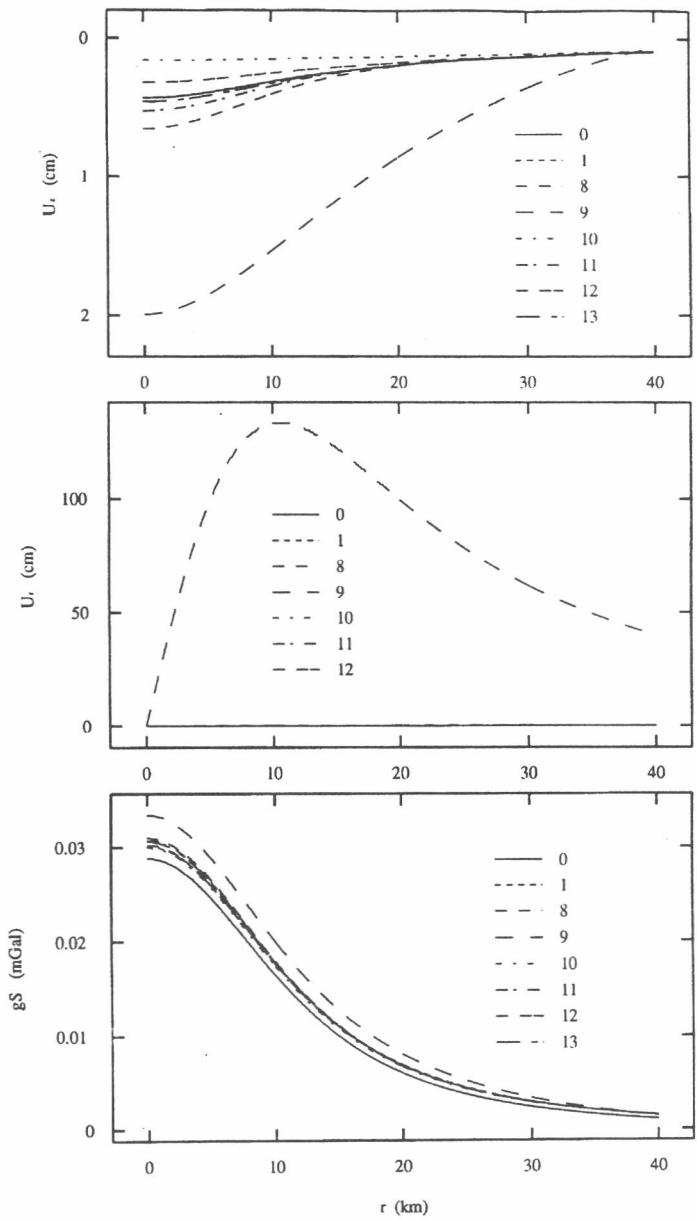

Figure 3. Vertical deformation U_z in cm, surface gravity change gS in mGal, and radial deformation U_r in cm, due to a point mass of 1 MU (10^{12} Kg) located at 15 km depth (layer 2) in media 0, 1 and 8 to 13 described in Table 1 (Fernández and Rundle, 1994a).

Data Set	ρ_1	ρ_2	ρ_3	λ_1	λ_2	λ_3	μ_1	μ_2	μ_3
0	Homogeneous half-space ρ=3.0, λ= μ=3.0								
1	3.0	3.0	3.0	3.0	3.0	3.0	3.0	3.0	3.0
2	2.5	2.5	3.0	3.0	3.0	3.0	3.0	3.0	3.0
3	3.0	1.5	3.0	3.0	3.0	3.0	3.0	3.0	3.0
4	3.0	6.0	3.0	3.0	3.0	3.0	3.0	3.0	3.0
5	1.5	2.5	3.0	3.0	3.0	3.0	3.0	3.0	3.0
6	6.0	4.5	3.0	3.0	3.0	3.0	3.0	3.0	3.0
7	D=20, ρ_1=2.5, ρ_2=3.0, λ_i= μ_i=3.0, i=1,2								
8	3.0	3.0	3.0	3.0	3.0	3.0	1.0	1.0	3.0
9	3.0	3.0	3.0	3.0	3.0	3.0	3.0	0.003	3.0
10	3.0	3.0	3.0	3.0	3.0	3.0	3.0	300.0	3.0
11	3.0	3.0	3.0	3.0	3.0	3.0	1.0	2.0	3.0
12	3.0	3.0	3.0	3.0	3.0	3.0	9.0	6.0	3.0
13	D=20, ρ_1= ρ_2=3.0, μ_1=2.5, μ_2=λ_i=3.0, i=1,2								

Table 1. Properties of the Media Considered in Figures 2 and 3. Equivalents for ρ are g/cm^3 =10^3 kg/m^3 and for λ and μ are10^{11} dyn/cm^2=10^{10} Pa (after Fernández and Rundle, 1994a).

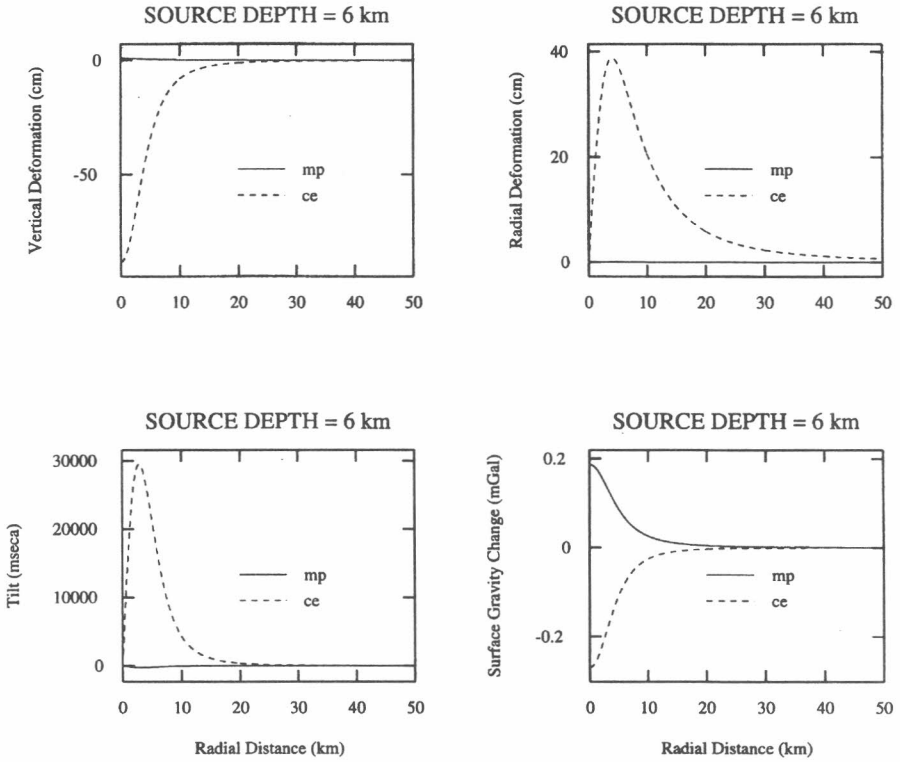

Figure 4. Vertical and horizontal deformation, tilt and surface gravity changes due to a center of expansion (ce) with a radius of 1 km and pressure of 10^4 bar, and a point mass (mp) of 1 MU located at 6 km depth in Lanzarote crustal model (Fernández et al., 1997).

(1995) show that the effects of gravity produce important differences in the displacement fields when long intervals of time are considered. Their model predicts the presence of a long wavelength component in the post-diking deformation field following a single event. Also, consideration of gravity field is necessary for computation of altitude changes with regard to an equipotential surface if we wish to obtain orthometric and geometric gravity gradients that are sensitive to the dynamics of the intrusion processes (*Rundle*, 1982a; *Fernández et al.*, 1997).

We have developed codes to compute the modeled effects. They are described by *Fernández and Rundle* (1994b) and *Fernández et al.* (1997). They can consider up to four layers over half-space, being named GRAVW PROGRAMS SET. Their characteristics are described in Table 2. The codes can be obtained via anonymous FTP from the server IAMG.ORG.

Also we calculate co- and postseismic surface displacements due to thrust faulting in a layered medium, including gravitational effects, composed of one elastic layer over a viscoelastic half-space (*Rundle*, 1981a, 1981b, 1982b; *Fernández et al.*, 1996a, 1996b), see Figure 5. A summary of the characteristics and parameters of the deformation model in this case can be seen in Table 3. Gravity arrests changes in the displacement fields after long periods of time. It can be observed, as a way of example, in Figure 6. This is important in using the model to analyze high-precision data from space geodetic techniques because inclusion of gravity is necessary to properly describe the time dependence of the displacement field.

	Gravw	Gravw1	Grav1	Gravw2	Gravw3	Gravw4
Number of Layers	1	1	2	2	3	4
Places where intrusion can be located	Layer	Anywhere	Anywhere	Anywhere	Anywhere	Anywhere
Computed Effects	u_z, g_s, g_B, g_{FA}, $d\phi$, SL	u_z, u_r, T, ε_z g_s, g_B, g_{FA} $d\phi$, SL	u_z, u_r g_s, g_B, g_{FA} $d\phi$	u_z, u_r, T, ε_z g_s, g_B, g_{FA} $d\phi$, SL	u_z, u_r, T, ε_z g_s, g_B, g_{FA} $d\phi$, SL	u_z, u_r, T, ε_z g_s, g_B, g_{FA} $d\phi$, SL

Table 2. List of codes forming GRAVW PROGRAMS SET describing number of layers considered in each one, possible locations of source and computed effects. u_z being vertical displacement, u_r being radial displacement, T denotes tilt, e_z is vertical strain, g_s, g_B and g_{FA} are surface, Bouguer and Free Air gravity changes respectively, $d\phi$ denotes potential change, and SL sea level changes. Codes are compared with other previous codes, GRAVW (Rundle, 1982) and GRAV1 (Fernández and Rundle, 1994a). Modified after Fernández et al. (1997).

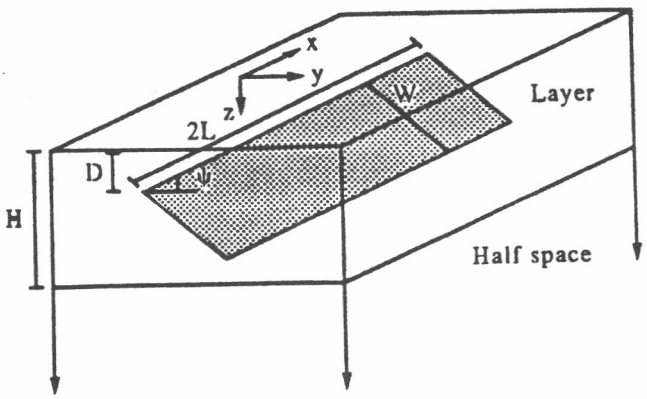

Figure 5. Geometry and coordinate system for a rectangular, finite, dipping fault in elastic-gravitational layer over a viscoelastic-gravitational half-space. D is depth, W is fault plane width, 2L is length along strike, Ψ is dip angle, and H is layer thickness (after Rundle, 1982a; Fernández et al., 1996b).

MODEL SUMMARY

EARTH MODEL: one layer over homogeneous half-space.		
LAYER:	PROPERTIES:	elastic-gravitational.
	PARAMETERS:	layer thickness, Lamé parameters and density.
HALF-SPACE:	PROPERTIES:	viscoelastic-gravitational.
	PARAMETERS:	Lamé parameters, density and relaxation type.
FAULT:	LOCATION:	layer.
	PARAMETERS:	depth, fault plane width, length along strike, dip angle (see Figure 5).
COORDINATE SYSTEM:	X AXIS:	parallel to the fault.
	Y AXIS:	perpendicular to the fault.
	Z AXIS:	vertical, positive inside the medium.
	ORIGIN:	center of the fault.

Table 3. Summary of the characteristics and parameters of the described deformation model (Fernández et al., 1996b).

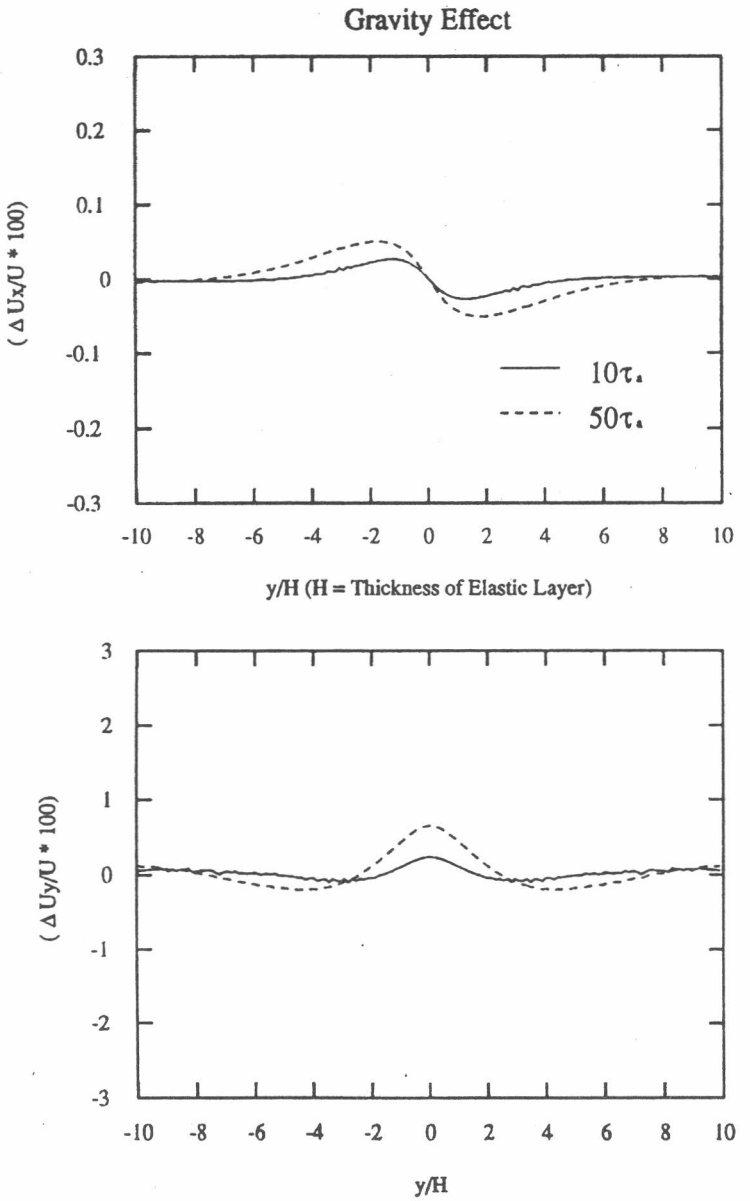

Figure 6. Viscoelastic-gravitational minus purely viscoelastic displacements (ΔU_x and ΔU_y) displacements, divided by dislocation U in the fault plane, due to a 90° dipping thrust fault in an elastic-gravitational layer over a viscoelastic-gravitational half-space at X = 10 km. Fault is 2L=30 km long, D = 0 km, W = 30 km, and H =30 km. 10 and 50τ_a are consided in this figure to show clearly the differences that appear after long periods of time. τ_a is the characteristic time defined by $\tau_a=2\eta/\mu_H$, where η is the viscosity of the Maxwell fluid (Fernández et al., 1996).

An important feature in the model is the long-wavelength postseismic displacement field, and this cannot be found in purely elastic models. The magnitude and wavelength of postseismic displacements grow as time elapses, see for example the case represented in Figure 7.

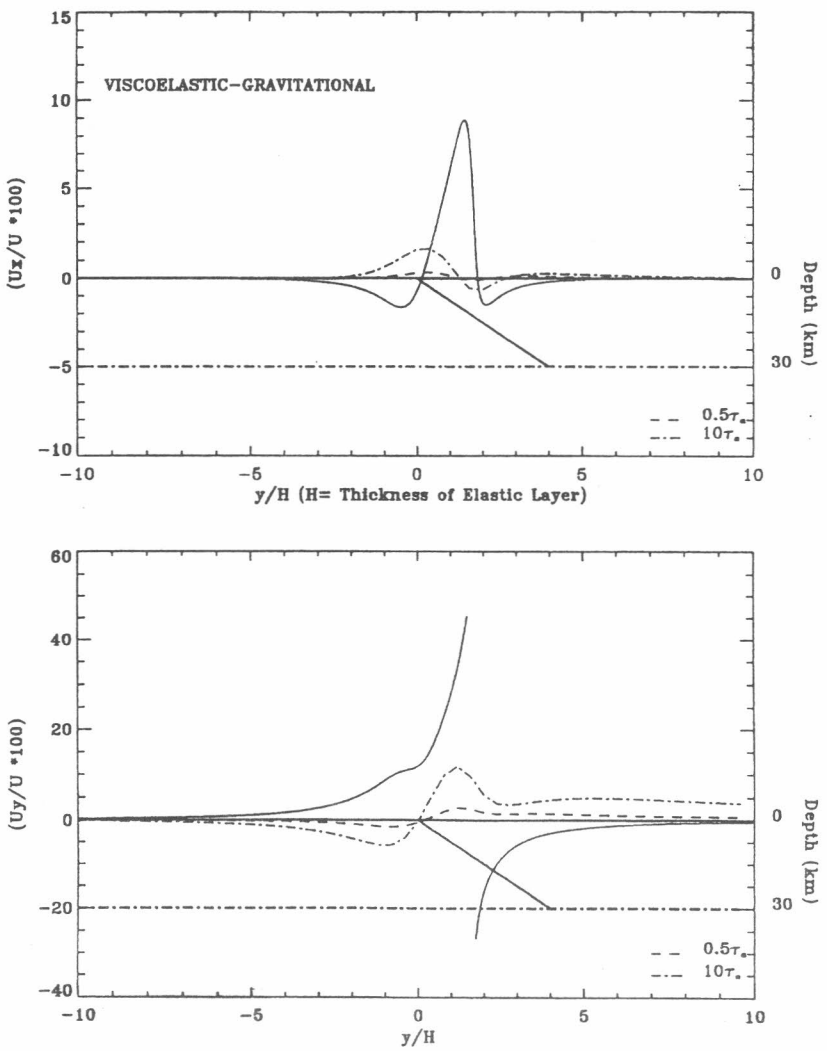

Figure 7. Surface horizontal displacements due to a 30° dipping thrust fault in an elastic-gravitational layer over a viscoelastic-gravitational half-space at X = 10 km. Fault is 2L = 30 km long, D = 0 km, W = 60 km, and H = 30 km (Fernández et al., 1996a).

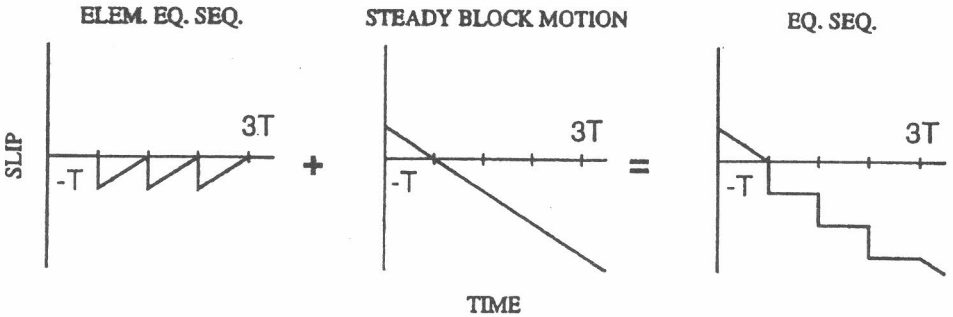

Figure 8. Diagram showing how an earthquake cycle (sequence) can be generated from superposition of an elementary cycle and steady block motion (after Savage and Prescott, 1978; Thatcher and Rundle, 1984; Fernández et al., 1996a).

One of the most important applications of the model presented here is the detailed examination of the time-dependent deformation of many earthquake cycles on the same fault plane, Figure 8. We have carried out earthquake cycle computations using the method described by *Cohen and Kramer* (1984) to compute components U_x, and U_y of displacement measured at time t, since an earthquake at t = 0 (*Fernández et al.*, 1996a). For models with a short recurrence time interval, the plate motion dominates the displacement field during the entire cycle, and major effects of the viscoelastic displacement only occur near the edge of the fault plane. However, for very long recurrence times, the accumulated viscoelastic displacement dominates the deformation field following the earthquake at large distances from the fault. This fact is can be observed in Figure 9.

Finally we have also calculated the postseismic surface displacements resulting from slip on a strike slip fault in an elastic layer overlying a viscoelastic half space (*Yu*, 1995; *Yu et al.*, 1996 a, 1996 b). An example of these computations is shown in Figure 10. The effects of gravity are found to produce minimal differences in the displacement fields near the fault.

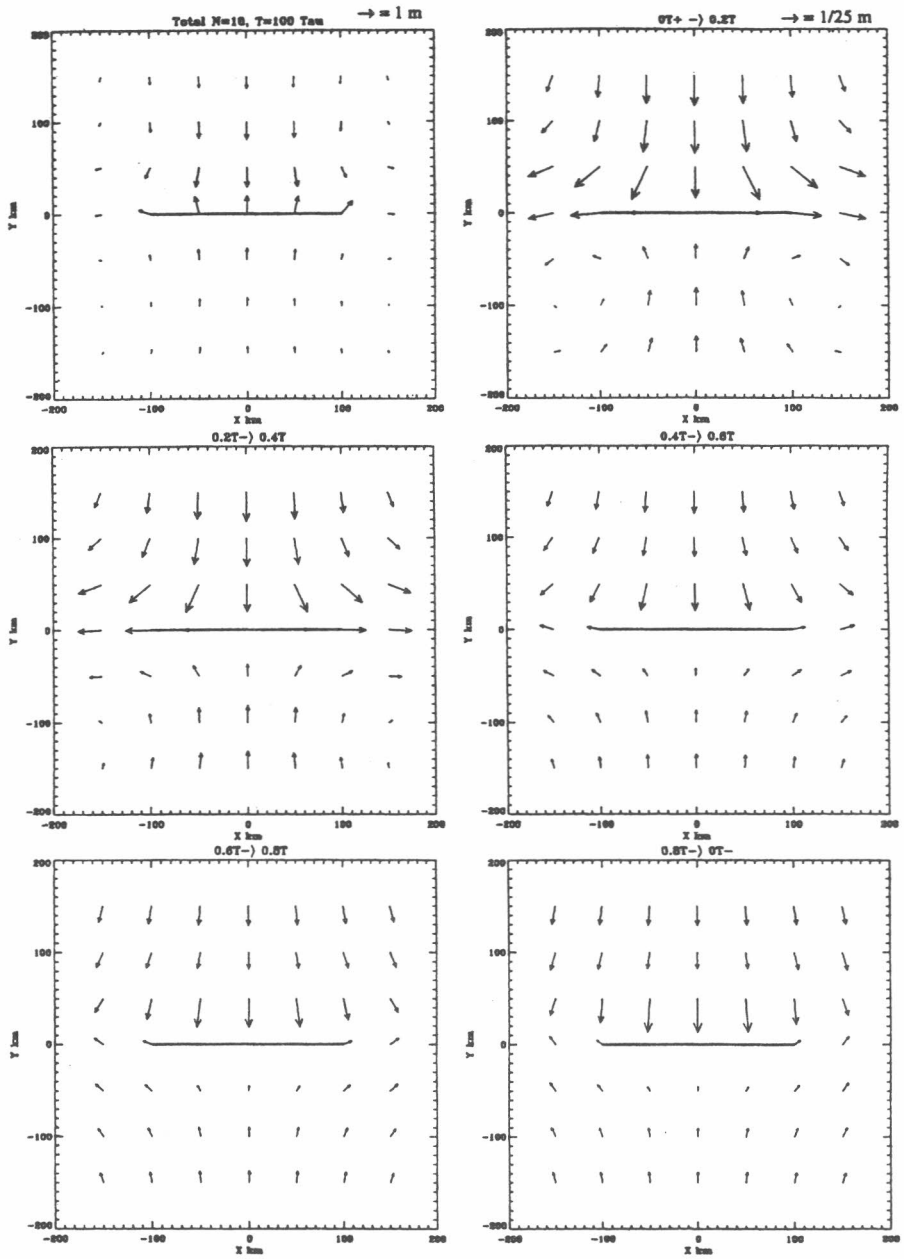

Figure 9. The accumulated displacement field due to 10 earthquakes prior to the event with recurrence time T=100 relaxation times. The thick line in the middle of the plot represents the fault. The coseismic displacement (top left) has its own scale. The rest of the charts use the same scale to represent the size of displacements. Except for the case of coseismic displacement, the size of the arrows is reduced by a factor of 25 (Fernández et al., 1996a).

At larger distances away from fault, the presence of gravity significantly changes the horizontal displacements due to a vertical strike slip fault, see Figure 11. For vertical displacement due to a dipping strike slip fault, gravity influences the magnitude as much as 40%. As with all layered viscoelastic calculations, our model predicts the presence of a long wavelength component in the postseismic deformation field following a single event that migrates with time (*Yu*, 1995; *Yu et al.*, 1996a).

The good fit between calculated results and GPS measurements at the Landers earthquake (*Shen et al.*, 1994) described by *Yu et al.* (1996a), Figure 12, suggest that viscoelasticity may be an important factor for strike slip events, just as it as for dip slip events. Vertical viscoelastic displacements are insignificant compared to coseismic displacements, but the horizontal co- and postseismic displacements have roughly the same magnitude. In this case it is possible to construct earthquake cycle models that, in certain circumstances (very long recurrence times, as for thrust faults), provide a means of identifying what stage of the earthquake cycle a given fault system is in.

The developed codes for computing displacements due to faulting are describe by Rundle (1981a), Fernández et al. (1996b) and Yu et al. (1996b). They can be obtain via anonymous FTP from the server IAMG.ORG (Computers & Geosciences) or from server FRACTAL.COLORADO.EDU (CIRES, University of Colorado at Boulder). In the last computer the codes can be found in the directory /fractal/users/ftp/pub/Viscocodes.

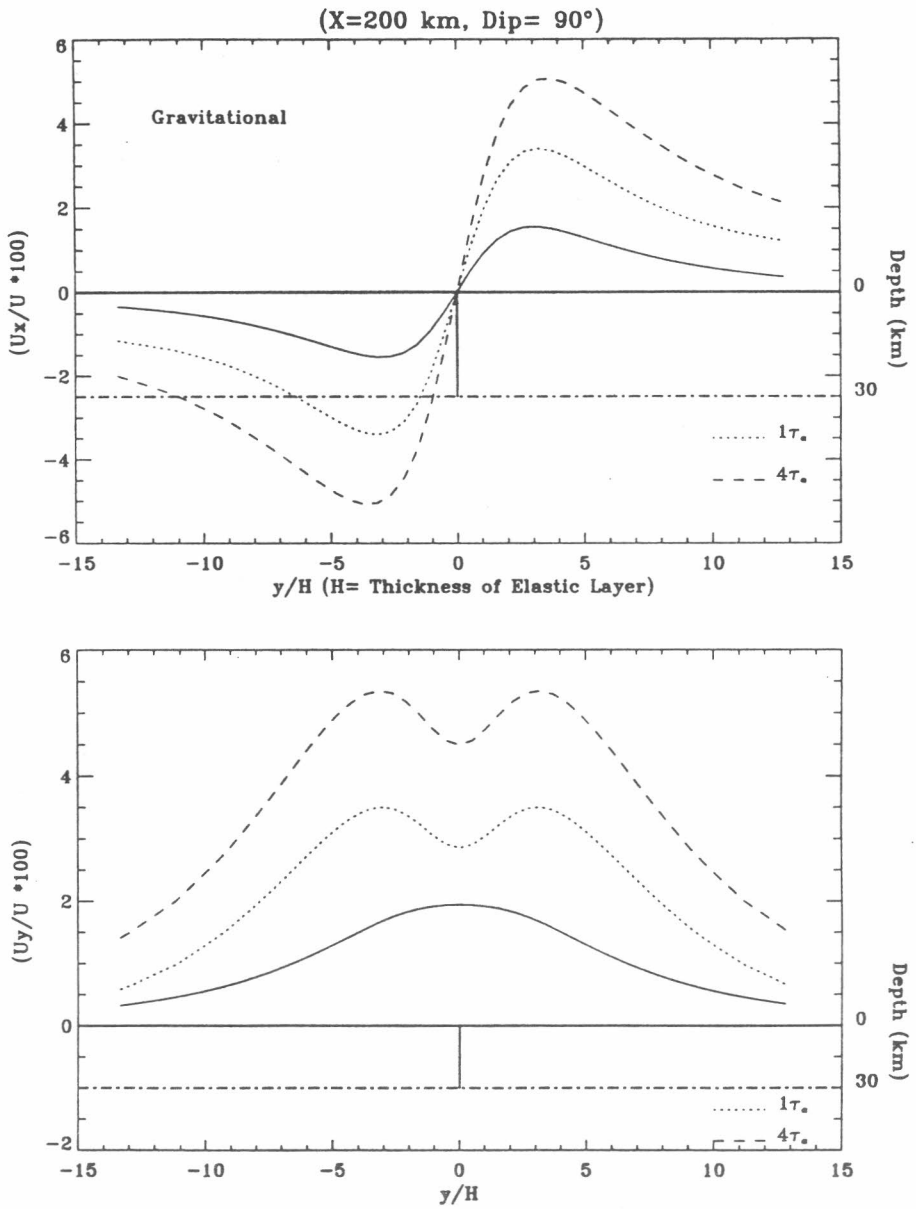

Figure 10. Surface displacements due to vertical strike-slip fault. Solid curve line is coseismic displacement and dashed curve lines represent the postseismic displacements. Horizontal dashed line is boundary of elastic layer and viscoelastic half-space at 30 km. Vertical short line represents fault line, which is vertical. Thick horizontal line is ground surface (Yu et al., 1996b).

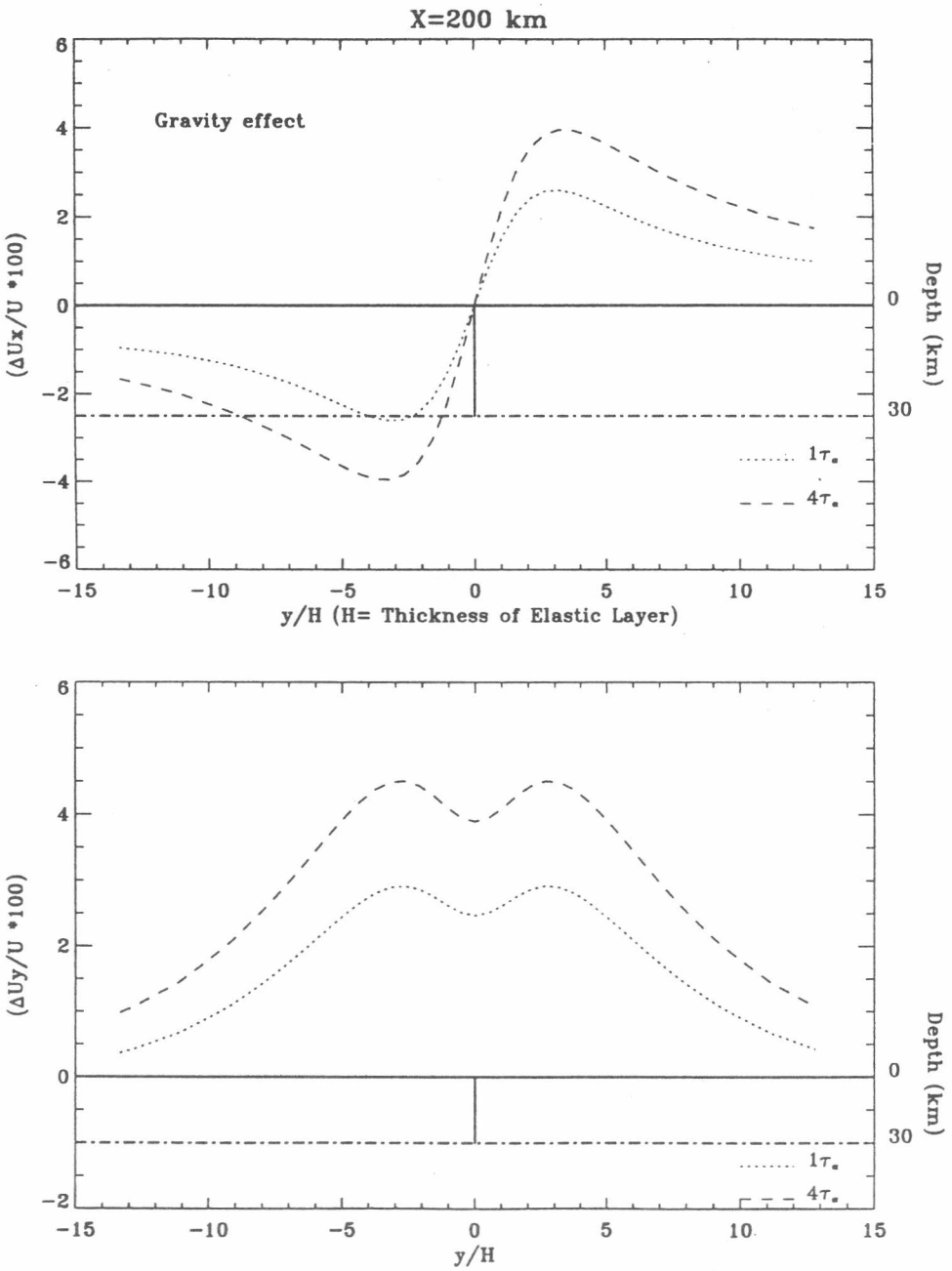

Figure 11. Difference of postseismic displacements, with and without gravity effects due to vertical strike-slip fault. Profile at 100 km of fault tip (Yu et al., 1996b).

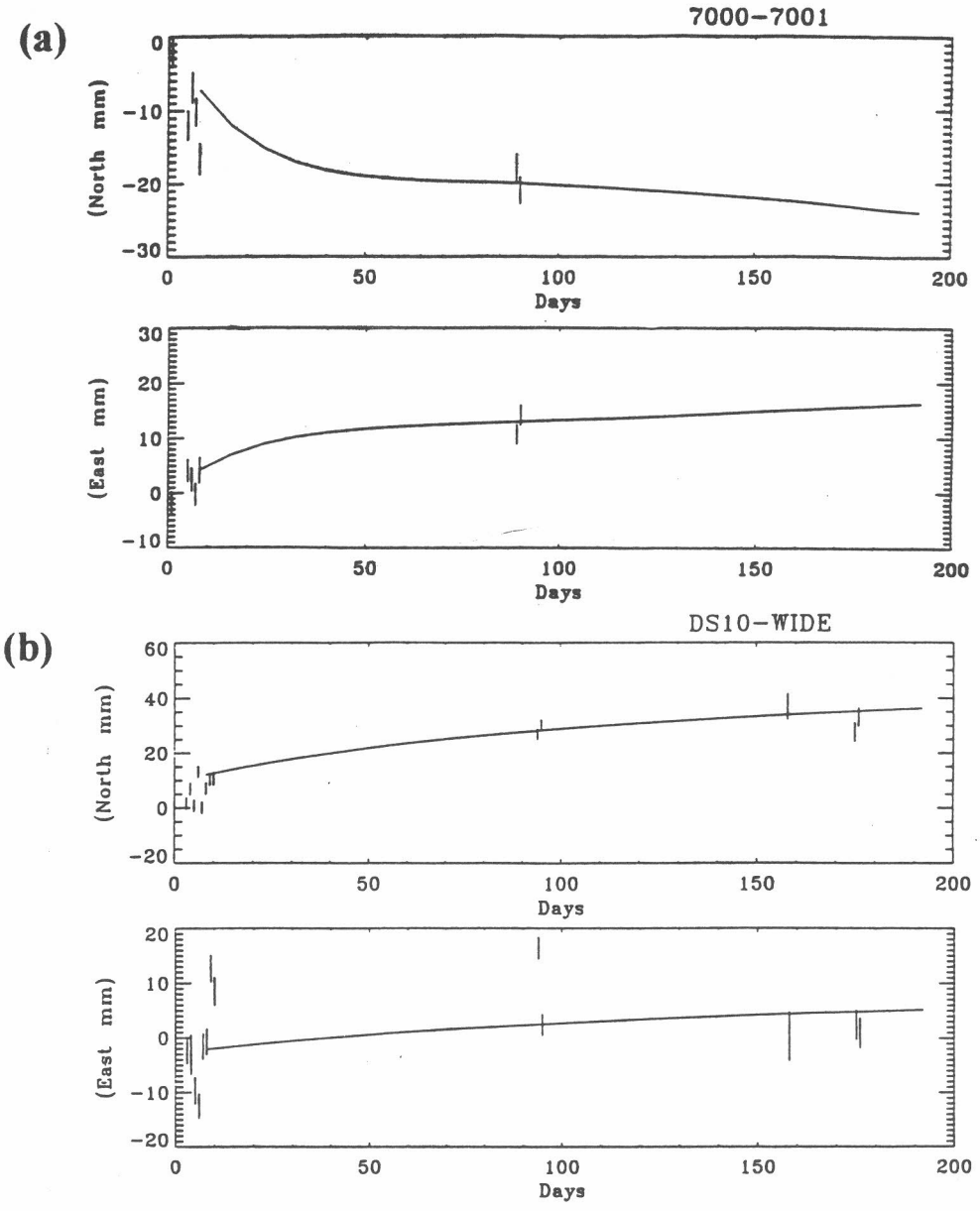

Figure 12. (a) Comparison between GPS data (vertical lines) and the computed results (solid line) for baseline 7000-7001, and (b) for baseline DS10-WIDE at the period of 200 days after main shock of the Landers earthquake in 1992 are shown (after Yu et al., 1996a). For more information and location of stations see Shen et al. (1994) and Yu et al. (1996a).

3. WORKS IN PROGRESS.

Among other topics, at present we are working on the extension of the model, considering a general number of layers in the general numerical formulation of the deformation model, including the possibility of viscoelactic, viscoelastic-gravitational and poro-elastic relaxation of the properties of layers and bottom half-space. This will be very useful in facilitating an appropiate interpretation of precise deformation data in both, the volcanic and faulting problem (see e.g. Bonafede et al., 1986).

We are also working on the consideration of different kind of magmatic intrusion on the modeling (spherical, ellipsoidal, etc), completing previous works such as Hofton et al. (1995).

The deformation model described for the volcanic problem is being applied to theoretically study the design of the most appropiate geodetic volcano monitoring system in the Canary Islands, Spain. The study involves two islands with different kinds of volcanism, namely Tenerife, where the Teide stratovolcano is located, and Lanzarote, with scattered centers of eruption and no major magmatic chamber between the edifices and the deep magma-generating areas (see e.g., Araña and Ortíz, 1991). Some preliminary results were described by Fernández and Díez (1995). Computation of strain and stress changes due to volcanic loading are also in progress.

Multilayered viscoelastic stress Green's functions are being developed for use in calculating Viscoelastic Coulomb Failure Functions (VCFF), and dynamic (time-evolutionary) General Earthquake Models, such as Virtual California simulations.

Computations of gravity changes produced by faulting with the described model will be carried out in the near future.

Another aspect of deformation model that we are working on is the application of techniques (Genetic Algorithm, GA) for solving the inverse problem. This is necessary for interpreting observed data on the basis of models and for validating the models. GA has been applied to invert the parameters of an earthquake rupture fault (Yu et al., 1997) using a simple model. Figure 13 shows the good match between observed data and the data obtained from model. Details about methodology, code and the example shown in Figure 13 can be found in Yu et al. (1997).

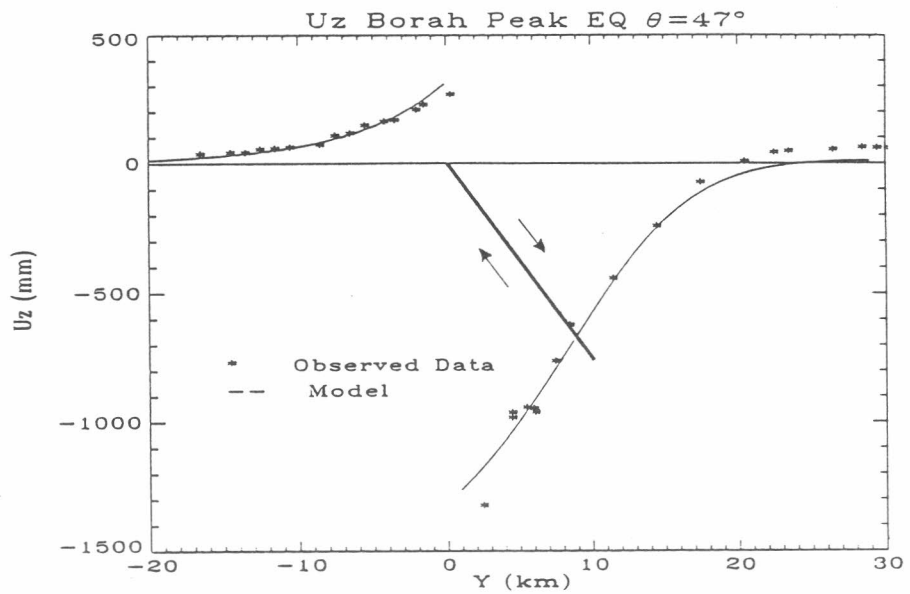

Figure 13. Vertical component leveling data (*) used for inverting the rupture parameters of the Borah Peak Earthquake, and result of the inverted model (solid curve). The thick line represents the ruptured fault plane, and arrows show the direction of the rupture (Yu et al., 1997).

Acknowledgments. Most of the previously described results were presented in the *First Meeting of Special Study Group 4.176 (Models of temporal variations of the Gravity Field) of the International Association of Geodesy* integrated into the 82nd session of Journées Luxembourgeoises de Géodynamique (Walferdange, Grand Duchy of Luxembourg, 17-19 March 1997). The recent research of J.F. has been supported by projects AMB96-0498-C04-04 and ENV4-CT96-0259 to Institute of Astronomy and Geodesy, Madrid, and contract NASA NAG5-3054 to CIRES. Ting-To Yu is supported by the postdoctoral research fellow grant of Institute of Earth Sciences, Academia Sinica. The research of John B. Rundle has been supported under US Department of Energy Grant number DE-FG03-95ER14499 to the Cooperative Institute for Research in Environmental Sciences (CIRES) at the University of Colorado at Boulder.

REFERENCES.

ARAÑA, V., AND R. ORTÍZ, The Canary Islands tectonic, magmatism and geodynamic framework. In A.B. Kampumzin and R.T. Lubala (Editors). *Magmatism in extensional structural settings. The Phanerozoic African plate.* Springer Berlag, Berlin, 209-249, 1991.

BEN-MENAHEM, A., AND S. J. SINGH, Multipolar elastic fields in a layered half space. *Bull. Seismol. Soc. Amer., 58,* 1519-1572, 1968.

BONAFEDE, M., M. DRAGONI, AND F. QUERINI, Displacement and stress fields produced by a centre of dilatation and by a pressure source in a viscoelastic half-space: application to the study of ground deformation and seismic activity at Campi Flegrei, Italy. *Geophys. J.R. Astron. Soc.*, 87, 455-485, 1986.

COHEN, S.C., AND M.J. KRAMER, Crustal deformation, the earthquake cycle, and models of viscoelastic flow in the asthenosphere. *Geophys. J.R. Astron. Soc.*, 78, 735-750, 1984.

COST, T.L., Approximate Laplace transform inversions in viscoelastic stress analysis. *AIAA J., 2* , 2157-2166, 1964.

FERNÁNDEZ, J., *Técnicas geodésicas y geodinámicas aplicadas a la investigación del riesgo volcánico en la isla de Lanzarote*. Ph. D. Thesis, Universidad Complutense de Madrid, 149 p., 1992.

FERNÁNDEZ, J., AND J. L. DÍEZ, Volcano monitoring design in Canary Islands by deformation model. *Cahiers Centre Européen de Géodynamique et de Séismologie*, 8, 207-217, 1995.

FERNÁNDEZ, J., AND J. B. RUNDLE, Gravity changes and deformation due to a magmatic intrusion in a two-layered crustal model. *J. Geophys. Res., 99*, 2737-2746, 1994a.

FERNÁNDEZ, J., AND J. B. RUNDLE, FORTRAN program to compute displacement, potential and gravity changes due to a magma intrusion in a multilayered Earth model. *Computers & Geosciences*, 20, 461-510, 1994b.

FERNÁNDEZ, J., T.-T. YU, AND J. B. RUNDLE, Horizontal viscoelastic-gravitational displacement due to a rectangular dipping thrust fault in a layered Earth model. *J. Geophys. Res.*, 101, 13581-13594, 1996a.

FERNÁNDEZ, J., T.-T. YU, J. B. RUNDLE, Deformation produced by a rectangular dipping fault in a viscoelastic-gravitational layered Earth model. Part I: Thrust fault. FLTGRV and FLRGRH FORTRAN programs. *Computers & Geosciences*, 22, 735-750, 1996b.

FERNÁNDEZ, J., J. B. RUNDLE, R. D. R. GRANELL, AND T.-T. YU, Programs to compute deformation due to a magma intrusion in elastic-gravitational layered Earth models. *Computers & Geosciences*, 23, 231-249, 1997.

GILBERT, F.; AND G. BACKUS, Propagator matrices in elastic wave and vibration problems, *Geophysics*; 31, 326-332, 1966.

HASKELL, N.A., The dispersion of surface waves on multilayered media. *Bull. Seismol. Soc. Amer.*; 43, 421-440, 1953.

HOFTON, M.A., J. B. RUNDLE, AND G. R. FOULGER, Horizontal surface deformation due to dike emplacement in an elastic-gravitational layer overlying a viscoelastic-gravitational half-space. *J. Geophys. Res.*, 100, 6329-6338, 1995.

LOVE, A.E.H., *Some Problems in Geodynamics*, 180 pp., Cambridge Univ. Press, New York, 1911.

RUNDLE, J.B., Viscoelastic crustal deformation by finite quasi-static source. J. Geophys. Res., 83, 5937-5945, 1978.

RUNDLE, J.B., Static elastic-gravitational deformation of a layered half-space by point couple sources, *J. Geophys. Res., 85*, 5355-5363, 1980.

RUNDLE, J.B., Numerical evaluation of static elastic gravitational deformation in a layered half-space by point couple sources, *Rep. 81-2058*, Sandia Nato. Lab., Albuquerque, N.M., 1981a.

RUNDLE, J.B., Vertical displacements from a rectangular fault in layered elastic-gravitational media, *J. Phys. Earth, 29*, 173-186, 1981b.

RUNDLE, J.B., Deformation, gravity, and potential changes due to volcanic loading of the crust, *J. Geophys. Res., 87*, 10729-10744, 1982a. (Correction, *J. Geophy. Res.*, v. 88, nº B12, p. 10647-10652, 1983)

RUNDLE, J.B., Viscoelastic-gravitational deformation by a rectangular thrust fault in a layered Earth, *J. Geophys. Res., 87*, 7787-7796, 1982b.

SCHAPERY, R.A., Approximate methods of transform inversion for viscoelastic stress analysis, *Proc. U.S. Natl. Congr. Appl. Mech., 4th*, 1075-1085, 1961.

SHEN, Z.K., D.D. JACKSON, Y. FENG, M. CLINE, M. KIM, P. FANG, AND Y. BOCK, Postseismic deformation following the Landers Earthquake, California, 28 June 1992. *Bull. Seismol. Soc. Amer., 84,* 780-791, 1994.

SINGH, S. J., Static deformation of a multilayered half space by internal sources, *J. Geophys. Res., 75,* 3257-3263, 1970.

THATCHER, W., AND J.B. RUNDLE, A viscoelastic coupling model for the cyclic deformation due to periodically repeated earthquakes at subdution zones, *J. Geophys. Res., 89,* 7631-7640, 1984.

THOMSON, W.T., Transmission of elastic waves throughout a stratified medium, *J. Appl. Phys., 21,* 89-93, 1950.

YU, T.-T., J. FERNÁNDEZ, AND J.B. RUNDLE, Inverting the parameters of an earthquake rupture fault with genetic algorithm. *Computers & Geosciences,* 1997 (In Press).

YU, T. T., *Crustal deformation due to dipping fault in elastic gravitational layer overlying viscoelastic gravitational half space: Models and applications*, Ph.D. dissertation, Univ. of Colo., Boulder, 1995.

YU, T.-T., J.B. RUNDLE, AND J. FERNÁNDEZ, Surface deformation due to strike slip fault in an elastic gravitational layer overlying a viscoelastic gravitational half space. *J. Geophys. Res.*, 101, 3199-3214, 1996a.

YU, T.-T., J.B. RUNDLE, AND J. FERNÁNDEZ, Deformation produced by a rectangular dipping fault in a viscoelastic-gravitational layered Earth model. Part II: Strike fault. STRGRV and STRGRH FORTRAN programs. *Computers & Geosciences*, 22, 751-764, 1996b.

YU, T.-T., AND S.-N. CHENG, Stress difussion and spatial migration of aftershocks in the Hualien area, Taiwan. *TAO*, 8, 31-48, 1997.